Dai et al. *NPG Asia Materials* (2022) 14:97
https://doi.org/10.1038/s41427-022-00449-6

NPG Asia Materials

ARTICLE Open Access

One-pot synthesis of stable antioxidant metal-ornamented polyphenol supramolecular assemblies for material engineering

Qiong Dai[1], Tong Shu[1], Huayan Yang[1], Lei Su[1], Xiaopeng Li[2] and Xueji Zhang[1]

Abstract

Natural polyphenols (NPPs) are of widespread interest in material engineering; however, only a small fraction of NPPs have been utilized in biomedical applications because of their poor solubility and instability in aqueous conditions. Herein, we report a family of metal-ornamented polyphenol supramolecular (MOPS) assemblies that are highly stable in aqueous solutions for over 6 months. In this one-pot, green synthesis method, metal ions are reduced in water by NPPs to form NPP-capped metal nanoclusters, which then assemble with more NPP molecules to form stable hydrophilic MOPS assemblies. This strategy is generally applicable to a range of NPPs (25 polyphenols tested) regardless of their original water solubility. The resulting stable MOPS assemblies, integrating attributes of both NPPs and metal nanoclusters, possess much stronger antioxidant capabilities than the NPPs, notably a multiplied capacity in superoxide-free radical scavenging capacity. MOPS assemblies can be further engineered, based on polyphenol chemistry, into various functional materials with potential for a wide range of antioxidant applications.

Introduction

Polyphenol-based supramolecular structures have attracted widespread interest due to their diverse properties, including their affinity for various materials endowed by their inherent phenolic chemistry, free radical scavenging capability imparted by the reducing nature of the phenolic hydroxyl groups and biocompatibility due to bioderived phenolic ingredients[1–5]. Such polyphenolic materials have been engineered with potential applications in catalysis, sensing, energy storage, biosynthesis, water purification, diagnosis, therapy, and tissue engineering[6–15]. Although natural polyphenols (NPPs) widely exist in various types of animals, plants, and microorganisms, their application in biomedical material engineering is limited by their instability in aqueous conditions, especially their sensitivity to oxidizing conditions[16]. Many NPPs with excellent chemical and biological activities have poor solubility in water[16–19]. For instance, the water solubility of curcumin (Cur), the major polyphenolic compound of the herb *Curcuma longa* with excellent bioactivity and health benefits, is 11 ng mL^{-1}, which limits its clinical applications[19]. In addition, many NPPs are sensitive to oxygen and light, especially when dispersed in water[16,18,19]. Therefore, organic solvents and additional stabilizers are generally used in the preparation of polyphenolic superstructures; however, those solvents and stabilizers can introduce additional toxicity or interfere with the desired functionality of the polyphenolic materials[17]. Polyphenolic polymers synthesized by conjugating dihydroxyphenyl (catechol) or trihydroxyphenyl (galloyl) groups on highly biocompatible polymers have been considered an appropriate replacement for NPPs in biomedical material engineering[3,20]. However, the synthesis process is typically labor intensive, involving

Correspondence: Tong Shu (shutong@szu.edu.cn) or Xueji Zhang (zhangxueji@szu.edu.cn)
[1]Guangdong Key Laboratory for Biomedical Measurements and Ultrasound Imaging, Guangdong Laboratory of Artificial Intelligence and Digital Economy (SZ), Shenzhen Key Laboratory for Nano-Biosensing Technology, School of Biomedical Engineering, Shenzhen University Health Science Center, Shenzhen, Guangdong 518060, China
[2]College of Chemistry and Environmental Engineering and Shenzhen University General Hospital, Clinical Medical Academy, Shenzhen University, Shenzhen, Guangdong 518060, China

organic solvents, multiple steps, and tedious purification[21,22]. In addition, harsh conditions are required in certain synthesis processes[23].

To enhance the stability and bioaccessibility of NPPs for biological and biomedical applications, stable inorganic nanostructures have been utilized to hybridize with polyphenolic materials. Therefore, a wide range of polyphenol-based organic/inorganic hybrid superstructures have been developed. For instance, tea polyphenol (TP), a mixture of polyphenols extracted from tea leaves, has been utilized to synthesize polyphenol-capped Ag and Au nanoparticles (NPs) with sizes ranging from 10 nm to a few hundred nanometers[24,25]. Similar to TP, different types of NPPs were extracted from plants and used for the synthesis of polyphenol-capped Au NPs with diverse sizes and shapes[26–28]. However, the synthesis of metal nanoclusters (NCs), which are multinuclear aggregates with sizes less than 3 nm and typical luminescence properties, catalytic activities, stability, and magnetism[29,30], by using NPPs in water has rarely been reported.

Herein, we report a family of metal-ornamented polyphenol supramolecular (MOPS) assemblies, which are hydrophilic nanoassemblies with NPP-capped metal NCs as ornaments and stable in aqueous conditions during long-term storage. In this one-pot and organic solvent-free synthesis process, NPPs are dispersed in water to reduce metal ions (Au^{III}, Cu^{II}, or Ag^{I}) and form NPP-capped metal NCs, followed by subsequent self-assembly of NPPs and NPP-capped metal NCs in water (Fig. 1), which produces hydrophilic MOPS assemblies with water solubility as high as 10^4–10^6 × compared to that of the NPPs. NPPs are chosen as both the reducing agents and protective ligands to stabilize the resulting metal NCs. The rate of reduction is controlled by varying the temperature of the reaction mixture. No organic solvents, specialized equipment, or additional steps are required in this process. The phenolic hydroxyl groups from NPPs play a key role in reducing metal ions and conjugating to metal NCs. Water-soluble NPP-protected metal NCs can adsorb and interact with other NPP molecules via, for example, hydrogen bonding, π–π stacking, and hydrophobic interactions and thus form stable MOPS assemblies in water (Fig. 1). The successful application and versatility of the present MOPS synthesis strategy is demonstrated with 25 different NPPs, resulting in a large family of MOPS assemblies and indicating that this method is generally applicable to NPPs with diverse numbers of phenolic hydroxyl groups regardless of their original solubility in water. The synthesized MOPS assemblies combine the advantages of their constituents—the metal NC ornaments (including stability and luminescence properties) and the NPP matrix (including reducibility and affinity to diverse materials)—with a multiplied free radical scavenging capacity and open up a new path for the engineering of functional metal/organic hybrid biomaterials.

Materials and methods

Synthesis of MOPS assemblies

The general synthesis of Au NC-ornamented polyphenol supramolecular (Au@NPP) assemblies is described as follows. NPPs (3 mg) were dispersed in 9.6 mL of ultrapure water in a 20 mL glass vial and mixed vigorously by a vortex mixer for 10 s. A freshly prepared aqueous solution of $HAuCl_4$ (25 mM, 0.4 mL) was then added to the dispersion. The reaction mixture was vigorously mixed by a vortex mixer for 60 s immediately after the addition of $HAuCl_4$. When tannic acid (TA), cyanidin (Cya), procyanidin B2 (PC-B), and procyanidin C1 (PC-C) were used as the NPP ligands, the reaction mixture turned

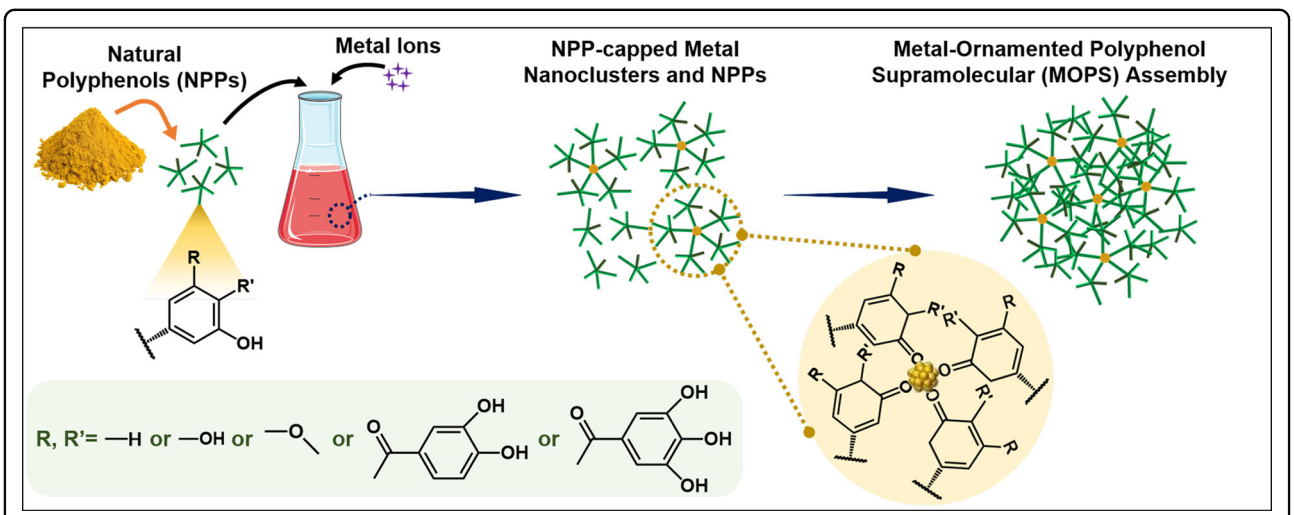

Fig. 1 Synthesis of MOPS assemblies. Schematic of the one-pot, green synthesis of MOPS assemblies.

brick red and was kept at 25 °C under gentle stirring for 10 min. For the remaining 21 types of NPP ligands, which were less soluble in water, the reaction mixture was heated to 75 °C to raise the reaction rate and shorten the reaction time under gentle stirring for 24 h. The reaction mixture was then centrifuged at 17,000 × *g* for 10 min. Large metal nanoparticles and aggregates, which were side products of the reduction reaction, could be removed from the reaction solution via high-speed centrifugation. After centrifugation, the supernatant was filtered with 220 nm diameter membranes to further remove the smaller nanoparticles and aggregates. The obtained Au@NPP solutions were then stored at 4 °C for at least 6 months with negligible changes observed in their optical properties. The supramolecular solutions were lyophilized to obtain yellowish Au@NPP powders. The synthesis of Ag NC- or Cu NC-ornamented polyphenol supramolecular assemblies was performed using the same procedure as described above except that $AgNO_3$ (25 mM, 0.4 mL) or $Cu(NO_3)_2$ (25 mM, 0.4 mL) solution was used, respectively, as the metal ion precursor.

Stability assessment

NPP and MOPS aqueous solutions were stored under ambient conditions for 1, 3, 5, 8, and 15 days or subjected to the following treatments: (i) heating, heated to 50 °C for 7 h; (ii) ultraviolet (UV) light irradiation, irradiated under 365 nm UV light for 7 h; (iii) acidification, adjusted to pH 2 and stored for 24 h; and (iv) basification, adjusted to pH 10 and stored for 14 h. Dynamic light scattering (DLS), ζ-potential, total polyphenol content measurement, and free radical scavenging capacity analyses of the MOPS solutions after storage or subject to the treatments were carried out as described in the Supplementary Information.

MOPS–metal–carbohydrate hydrogel fabrication

In a typical synthesis, to obtain a carboxymethyl chitosan (CMCS)–Au@TA–Ti^{IV} sol, 500 μL of CMCS solution (5 wt.% in water) was introduced into a 2 mL glass vial. Then, 2.2 μL of Ti^{IV} solution (50 wt.% in water) was added to 500 μL of Au@TA solution (1.5 mM in water) in a 1.5 mL tube with vigorous vortexing for 1 min to obtain the orange–red Au@TA–Ti^{IV} mixture. The Au@TA–Ti^{IV} mixture (500 μL) was then added to the CMCS solution in a glass vial with vigorous vortexing for 1 min. The mixture was left to stand. An orange–red gel formed within 5 min, as confirmed by the vial inversion test. Additional gelation tests were performed using Au@Cur, Au@gallic acid (GA), or Au@caffeic acid (CA) and Zr^{IV}.

MOPS-based metal–phenolic network (MPN) core–shell particle and capsule assembly

All solutions were freshly prepared. In a typical synthesis, 300 μL of polystyrene (PS) particles (2.5 wt.% in water) was first added to 570 μL of water. Then, 30 μL of $FeCl_3$ solution (5 mg mL^{-1} in water) was added, and the dispersion was vortexed for 10 s. Immediately, 600 μL of Au@TA solution (1 mg mL^{-1} in water) was added followed by vigorous vortexing for 10 s. Phosphate-buffered saline (PBS) buffer (1.5 mL, 100 mM, pH 8.0) was then added, and the dispersion was vortexed for 1 min. The particles were washed with 3 mL of ultrapure water three times to remove excess Au@TA and Fe^{III}. In the washing step, the particles were centrifuged (5000 × *g*, 5 min), the supernatant was discarded, and the pellets were vortexed for 10 s. To obtain capsules, the PS cores were removed by washing with tetrahydrofuran (THF) three times. In each THF washing step, the pellets were first vortexed for 10 s, 2 mL of THF was added to the pellet, and the pellet was then resuspended through gentle pipetting (at least 20×). This suspension was then kept on a gentle rotating mixer for 30 min. The particles were centrifuged (5000 × *g*, 10 min), the supernatant was removed, and the process was repeated three times. After the final THF washing step, the pellet was resuspended in 2 mL of ultrapure water through gentle pipetting.

Results and discussion

We first demonstrated the synthesis of gold nanoclusters (Au NCs) using Cur, a nonflavonoid polyphenol compound with poor solubility (11 ng mL^{-1}) and stability in water[19]. Cur and Au^{III} were mixed thoroughly in water. The mixture could be warmed up to 75 °C to increase the reaction rate. The reaction was allowed to proceed for 24 h. Transmission electron microscopy (TEM) analysis showed that the obtained aqueous solution of Au-ornamented Cur supramolecular (Au@Cur) assemblies formed an amorphous film when added dropwise onto the copper grid, whereas ordered lattice structures were detected within the amorphous film under high-resolution TEM imaging (Fig. 2a). The lattice fringes were measured to be 2.35 Å, which was identical to the (111) lattice of face-centered cubic (FCC) Au. The presence of Au ornaments in the synthesized supramolecular assemblies was confirmed by energy-dispersive X-ray spectroscopy (Fig. S1). These results indicated the feasibility of engineering highly ordered materials from amorphous NPP films with the assistance of Au NC formation. The aqueous solution of the synthesized Au@Cur assemblies (1 mg mL^{-1}) was transparent, which was nearly colorless under ambient light and exhibited blue fluorescence under 365 nm UV light (Fig. 2b). Fluorescence spectra showed the luminescence properties of Au@Cur assemblies in water (Fig. 2c). The Au@Cur assemblies showed maximum emission at ~450 nm with excitation at ~350 nm, which was different from the emission of natural Cur at ~550 nm with the same excitation light (Fig. 2c and Fig. S2). Based on the fluorescence intensity of the synthesized product, the synthesis conditions of Au@Cur

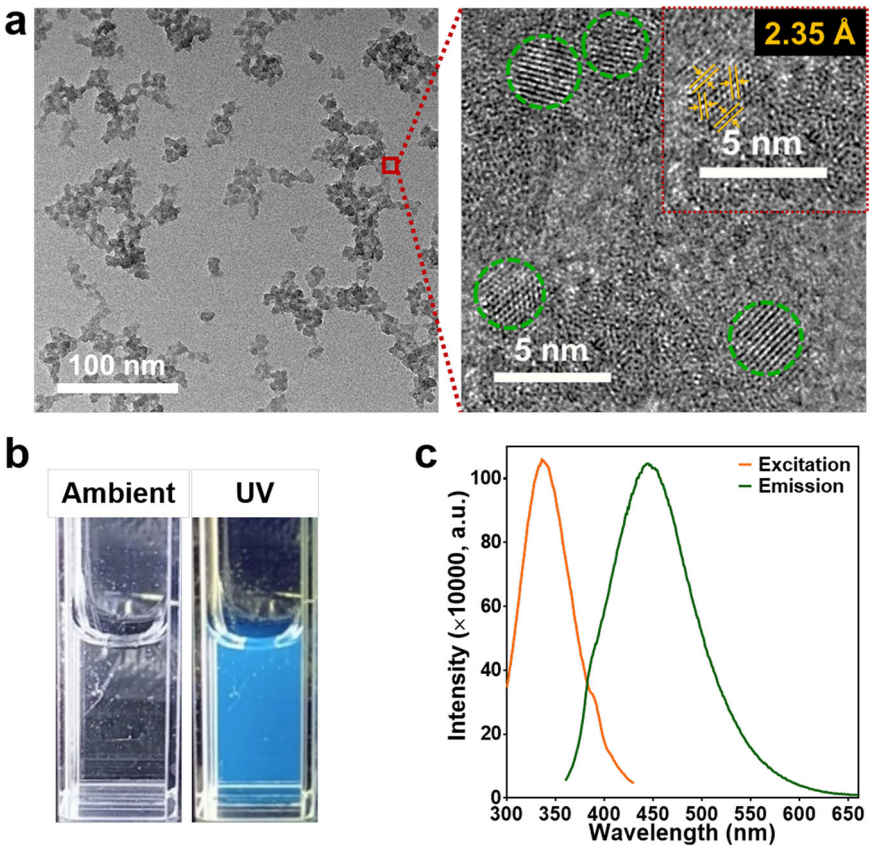

Fig. 2 Characterization of Au@Cur assemblies. a Low- and high-resolution TEM images of Au@Cur. The inset with a red dashed frame is an enlarged high-resolution TEM image of the crystalline region. **b** Photograph of Au@Cur aqueous solution under ambient light and UV light. **c** Fluorescence spectra of Au@Cur aqueous solution.

assemblies could be optimized to obtain products with efficient luminescent emission (Fig. S2).

UV–visible (UV–vis) spectrophotometry and Fourier transform infrared (FTIR) spectroscopy revealed the differences in the molecular structures of the synthesized Au@Cur and natural Cur (Fig. 3a and Fig. S3). Natural Cur showed two distinct absorption bands in the UV–Vis spectrum at 250–280 and 420–450 nm, related to the n–π* and π–π* transitions, respectively. However, for the synthesized Au@Cur, the absorption band at 420–450 nm disappeared, while the absorption band attributed to the n–π* transition was less affected. In addition, there was no absorption peak in the 520–560 nm region, which is typical for Au NPs due to their surface plasma resonance properties, for the Au@Cur sample, indicating the absence of Au NPs in the Au@Cur solution. In the FTIR spectrum, the synthesized Au@Cur assemblies showed a much higher and broader absorption band at 3600–3100 cm^{-1} compared to natural Cur, which could be attributed to the O–H stretching of phenolic hydroxyl groups[31,32]. The broadening of this band indicated that the phenolic hydroxyl groups of Cur ligands participated in the assembly of Au@Cur assemblies via intermolecular hydrogen bonds[31]. The hydroxyl groups of Cur reduced Au^{III} to Au^{0}, while Cur ligands capped the synthesized Au NCs, forming Cur-covered Au NCs. The reduction of the total polyphenol content in Au@Cur compared with the total polyphenol content in Cur confirmed the consumption of the hydroxyl groups during the synthesis of Au NCs (Fig. 3b and Fig. S4). The Cur-capped Au NCs then adsorbed unreacted Cur and subsequently assembled into supramolecular assemblies with a considerably higher free phenolic hydroxyl activity, as indicated by the FTIR spectra[31,32]. The complete disappearance of the absorption band at 420–450 nm, a typical indicative band of Cur, for the synthesized Au@Cur in the UV–Vis spectrum demonstrated that there were no free Cur molecules left in the final product. DLS analysis revealed the distribution of the Au@Cur assemblies in different aqueous solutions (Fig. 3c and Fig. S5). The diameter of Au@Cur assemblies in ultrapure water was 81 ± 4 nm and was hardly affected by the pH or salt concentration of the aqueous solutions.

Unlike hydroalcohol solutions of natural Cur that are not stable when stored in ambient environments (Fig. S6),

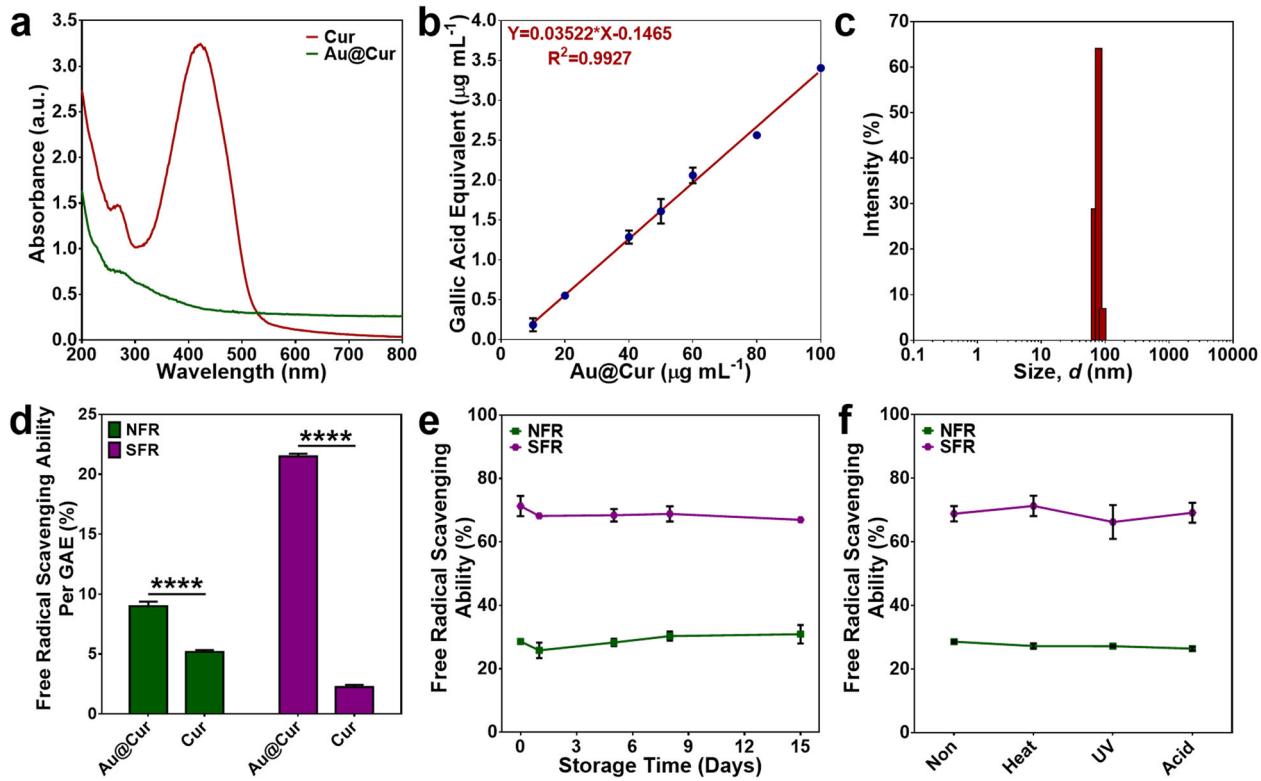

Fig. 3 Properties of Au@Cur assemblies. a UV–Vis absorbance spectra of Cur and Au@Cur. **b** Standard curve of the total polyphenol content of Au@Cur. **c** Size distribution of Au@Cur dissolved in ultrapure water. **d** Free radical scavenging capacities of the synthesized Au@Cur and natural Cur. Stability of free radical scavenging capacities of the as-prepared Au@Cur aqueous solutions after storage at ambient temperature for various time periods (**e**) or after being subjected to different treatments (**f**). NFR nitroxide free radical; SFR superoxide free radical. $n = 3$, $^{****}p < 0.0001$, nonparametric one-way ANOVA.

Au@Cur solutions (1 mg mL^{-1}) were highly stable when stored under ambient conditions, with neither a color change nor precipitation observed for up to 6 months. DLS analysis confirmed the physical stability of the Au@Cur aqueous solutions either stored under ambient conditions for different time intervals or subjected to various treatments (Fig. S7). Moreover, Au@Cur assemblies maintained chemical stability in aqueous solutions without changes observed in their total polyphenol content when either stored under ambient conditions for a long period or subjected to heating, UV irradiation, or acid treatment (Fig. S8). These results indicated that the incorporation of metal ornaments into the NPP supramolecular assemblies could largely increase the stability of the NPP-based nanoassemblies. However, similar to NPPs, the phenolic hydroxyl groups of the synthesized Au@Cur assemblies were vulnerable to basic conditions. The total polyphenol content of Au@Cur decreased sharply in basic solutions with a pH higher than 10. Therefore, strong alkali conditions should be avoided during the storage and processing of MOPS assemblies.

NPPs are generally recognized as efficient antioxidants that scavenge free radicals and inhibit the risks of oxidative stress[33,34]. A commonly used method to assess antioxidant ability is to measure the free radical scavenging capacity of antioxidants. In this work, the free radical scavenging capacities of natural Cur and the synthesized Au@Cur were determined by using different free radical scavenging capability determination kits (Fig. 3d–f and Fig. S9). At equal total polyphenol content levels (per gallic acid equivalent (GAE)), Au@Cur possessed a much higher free radical scavenging capacity than natural Cur (Fig. 3d). Specifically, Au@Cur exhibited doubled nitroxide free radical (NFR) scavenging capacity and almost 10-fold enhanced capability for superoxide free radical (SFR) scavenging. Moreover, the free radical scavenging capacities of Au@Cur remained constant during long-term storage under ambient conditions as well as under various treatments (Fig. 3e, f). Compared to natural Cur, the introduction of Au NCs to Au@Cur assemblies could be a key factor resulting in enhanced and more stable capacities for free radical scavenging. The detailed mechanisms are currently under investigation to determine whether there are any combined or synergistic effects between the Au NCs and Cur ligands.

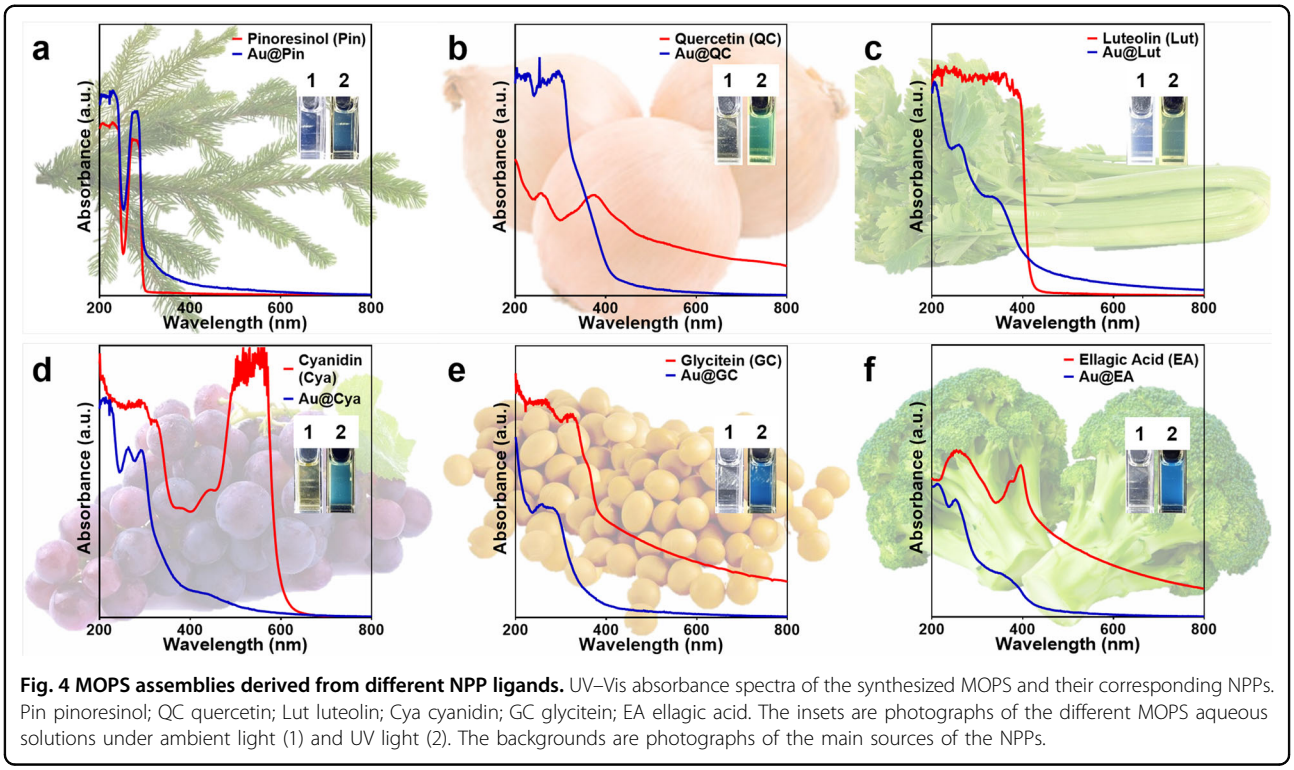

Fig. 4 MOPS assemblies derived from different NPP ligands. UV–Vis absorbance spectra of the synthesized MOPS and their corresponding NPPs. Pin pinoresinol; QC quercetin; Lut luteolin; Cya cyanidin; GC glycitein; EA ellagic acid. The insets are photographs of the different MOPS aqueous solutions under ambient light (1) and UV light (2). The backgrounds are photographs of the main sources of the NPPs.

To demonstrate the general applicability of this one-pot, organic solvent-free MOPS synthesis method to diverse NPPs, 24 other NPP compounds (Fig. S10) were examined to synthesize the corresponding MOPS assemblies. The resulting UV–Vis spectra showed the differences observed in the absorption spectra of the MOPS assemblies and NPPs, suggesting an alteration in the molecular structure of the synthesized MOPS assemblies (Fig. 4 and Fig. S11). The luminescence properties of the series of synthesized MOPS assemblies were different due to the different ligands from which MOPS assemblies were derived (Fig. S12). In addition to Au, Ag, and Cu were examined to synthesize the corresponding Ag NC- and Cu NC-ornamented supramolecular assemblies. Using Cur, Ag^{I} and Cu^{II} were reduced in water to form Cur-capped Ag NCs and Cu NCs, which subsequently assembled into the corresponding MOPS (Ag@Cur and Cu@Cur) assemblies (Fig. 5). Because of the different types of metal NC ornaments, Ag@Cur and Cu@Cur assemblies exhibited different light absorption and luminescence properties (Fig. 5a, b, d, e). There were three absorption peaks in the range of 200–350 nm for Ag@Cur assemblies, while there were only two absorption bands in the same region for Cu@Cur assemblies. In addition, the maximum emissions of Ag@Cur and Cu@Cur assemblies were at ~500 and ~450 nm, respectively, with excitation at ~350 nm. All these results indicated that the metal ornaments, although at a low content in the MOPS assemblies, played an important role in determining the microstructures and physiochemical properties of the supramolecular assemblies. Similar to Au@Cur, ordered lattice structures were detected within the amorphous Ag@Cur and Cu@Cur films, suggesting that metal NCs could mediate the fabrication of highly ordered structures from amorphous polyphenol assemblies (Fig. 5c, f). The lattice fringes of the Ag@Cur and Cu@Cur samples were measured to be 2.36 and 2.05 Å, respectively, which were attributed to the (111) lattice of the FCC Ag and the (111) lattice of the FCC Cu. Moreover, similar to Au@Cur assemblies, Ag@Cur and Cur@Cur assemblies showed significantly higher capacities in scavenging SFRs than natural Cur at equal total polyphenol content levels (Fig. S13). This indicated that the presence of metal NC ornaments could not only stabilize the polyphenolic ligands but also remarkably enhance the antioxidant capacities of polyphenols.

For NPPs with poor aqueous solubility, e.g., Cur, ellagic acid (EA) and quercetin (QC), continuous synthesis of MOPS was achieved through the addition of supplementary metal ions into the reaction mixture (Fig. 6a–f). By controlling the synthesis time and cycle number, the composition of the synthesized assemblies, indicated by the UV–Vis absorption and fluorescence intensity, could be tuned (Fig. S14). For NPPs with poor solubility in water, the reaction mixture could be heated to accelerate the synthesis of metal NCs by increasing both the amount of NPP ligands in water and the oxidation–reduction rate. In addition, the

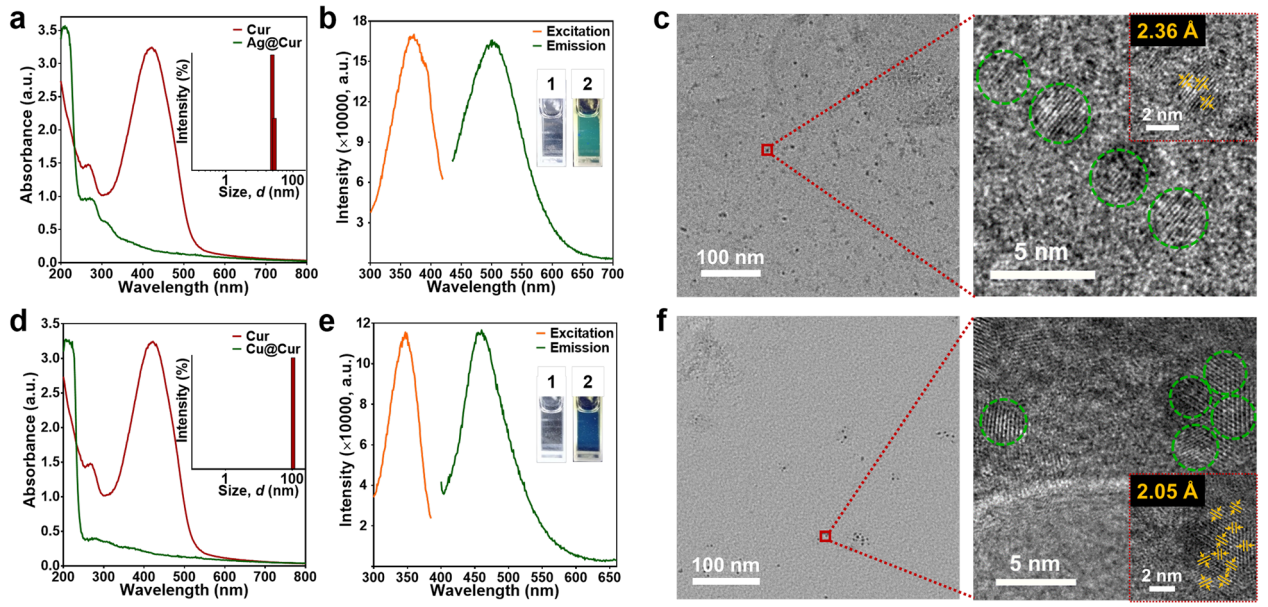

Fig. 5 Synthesis of MOPS assemblies using different metal ions. UV–Vis spectra (**a**, **d**), fluorescence spectra (**b**, **e**), and TEM images (**c**, **f**) of Ag@Cur (**a**–**c**) and Cu@Cur (**d**–**f**). Insets in (**a**) and (**d**) are the size distributions of Ag@Cur and Cu@Cur in water. Insets in (**b**) and (**e**) are photographs of MOPS aqueous solutions under ambient light (1) and UV light (2). Insets in (**c**) and (**f**) with red dashed frames are the enlarged high-resolution TEM images of the crystalline regions.

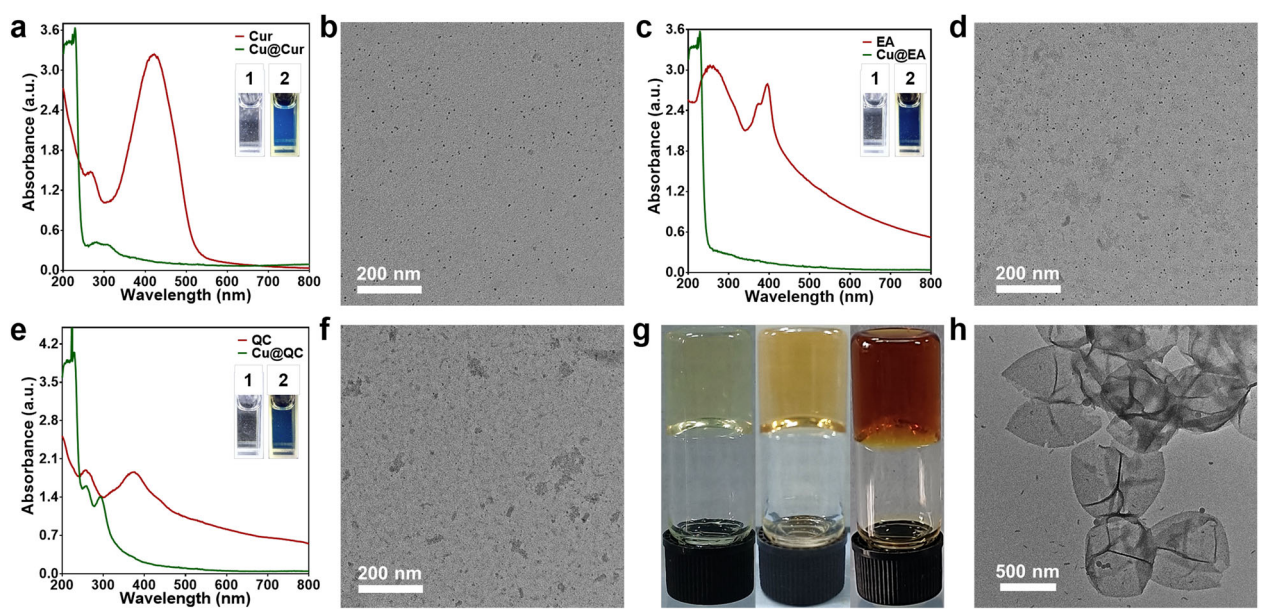

Fig. 6 MOPS assemblies synthesized in three synthesis cycles and functional material engineering using MOPS assemblies. a–f UV–Vis absorbance spectra and TEM images of Cu@Cur (**a**, **b**), Cu@EA (c, d), and Cu@QC (**e**, **f**) synthesized in three synthesis cycles. **g** Photographs of hydrogels formed by Au@Cur, Zr^{IV}, and carboxymethyl chitosan (CMCS) (left); Au@CA, Zr^{IV}, and CMCS (middle); and Au@GA, Ti^{IV}, and CMCS (right). CA caffeic acid; GA gallic acid. **h** TEM image of hollow Au@TA–Fe^{III} capsules. Insets in (**a**) and (**d**) are the size distributions of Ag@Cur and Cu@Cur in water. Insets in (**a**), (**c**), and (**e**) are photographs of MOPS aqueous solutions under ambient light (1) and UV light (2).

synthesized NPP-capped metal NCs could "pull" more NPP molecules into water from the undissolved NPP solids to form hydrophilic MOPS assemblies, thereby increasing the solubility of the NPPs in water. Continuous synthesis could allow for a relatively complete reaction of NPPs and reduce the waste of raw materials.

Moreover, in the present study, continuous synthesis of MOPS assemblies enabled the mass production of hydrophilic polyphenolic supramolecular nanostructures. For NPPs with good solubility in water, such as TA, TP, and procyanidins, the reaction proceeded rapidly, with more polyphenol molecules dissolved and interacting with metal ions in water. Therefore, the synthesis process was completed at ambient temperature within 15 min. Mass production of MOPS by using such soluble NPPs could be achieved by increasing the amount of reactants in the reaction system proportionately. In addition, the fluorescence intensity of the synthesized MOPS could be tuned by adjusting the ratio of the reactants in the reaction system (Fig. S15).

With a relatively high content of active phenolic hydroxyl groups, MOPS assemblies possess many physicochemical properties that are similar to NPPs, including metal chelation and affinity for different materials. These polyphenolic properties, based on polyphenol chemistry, enabled the NPPs to be utilized as building blocks for the engineering of a wide range of nanostructured functional materials, including MPN-based nanoparticles, nanocapsules and hydrogels[2–6]. Similarly, MOPS assemblies with polyphenolic properties could be engineered into different functional materials via polyphenol chemistry, e.g., surface coatings, hollow structured capsules, hydrogels, and colloidal suspensions (Fig. 6g, h and Fig. S16). Owing to their excellent free radical scavenging capacity, these MOPS-based materials are expected to be excellent antioxidants for a wide range of biomedical applications. Free radicals, especially reactive oxygen species (ROS), are typically associated with oxidative stress in the body and are related to the development of many diseases, including cardiovascular diseases, neurological disorders, obesity, aging, and cancer[35–39]. Antioxidants are able to reduce free radicals, especially ROS, alleviate oxidative stress in the body and prevent or treat related disorders. Therefore, these MOPS-based materials are anticipated to have potential in various areas, including the diagnosis and treatment of various diseases.

Conclusion

In summary, the family of stable antioxidant MOPS assemblies reported herein, prepared via the simple one-pot and green method, provides a generally applicable solution to increase the hydrophilicity and stability of NPPs. The MOPS assemblies integrate the advantages of both the metal NCs and NPPs, resulting in a range of metal/organic nanocomplexes with excellent stability, luminescence properties, free radicals, especially SFR scavenging capacity, and extensive affinity for biomolecules. The synthesized NPP-derived MOPS assemblies presented in this study expand the library of advanced metal/polyphenol hybrid nanomaterials that may be used in a wide range of biological and biomedical applications.

Acknowledgements

This research was funded by the National Natural Science Foundation of China (Q.D., 21802088; T.S., 21904011; T.S. and X.Z., 21890742, 21727815, and 82061138005). T.S. acknowledges support from the Shenzhen Science and Technology Innovation Commission (20200809233237001). We thank the Instrument Analysis Center of Shenzhen University for assistance with TEM analysis. We thank Associate Professor Yizhen Liu at the College of Chemistry and Environmental Engineering of Shenzhen University for the collaboration and assistance with necessary experimental supplies. We acknowledge Professor Frank Caruso at The University of Melbourne and Dr. Yan Yan Shery Huang at University of Cambridge for their necessary discussion and intellectual input.

Author contributions

Q.D. and T.S. conceived the idea. Q.D. designed the experiment, conducted the experiments and data analysis, and wrote the manuscript. H.Y., L.S., and X.L. assisted with the writing and revision of the manuscript. X.Z. supervised the project. All authors have given approval to the final version of the manuscript.

Competing interests

The authors declare no competing interests.

Publisher's note

Springer Nature remains neutral with regard to jurisdictional claims in published maps and institutional affiliations.

Supplementary information The online version contains supplementary material available at https://doi.org/10.1038/s41427-022-00449-6.

Received: 3 September 2022 Revised: 21 October 2022 Accepted: 27 October 2022.
Published online: 16 December 2022

References

1. Sileika, T. S., Barrett, D. G., Zhang, R., Lau, K. H. A. & Messersmith, P. B. Colorless multifunctional coatings inspired by polyphenols found in tea, chocolate, and wine. *Angew. Chem. Int. Ed.* **52**, 10766–10770 (2013).
2. Rahim, M. A. et al. Metal-phenolic supramolecular gelation. *Angew. Chem. Int. Ed.* **55**, 13803–13807 (2016).
3. Dai, Q., Geng, H., Yu, Q., Hao, J. & Cui, J. Polyphenol-based particles for theranostics. *Theranostics* **9**, 3170–3190 (2019).
4. Pan, S. et al. Exploiting supramolecular dynamics in metal-phenolic networks to generate metal-oxide and metal-carbon networks. *Angew. Chem. Int. Ed.* **60**, 14586–14594 (2021).
5. Ejima, H. et al. One-step assembly of coordination complexes for versatile film and particle engineering. *Science* **341**, 154–157 (2013).
6. Guo, J. et al. Engineering multifunctional capsules through the assembly of metal-phenolic networks. *Angew. Chem. Int. Ed.* **53**, 5546–5551 (2014).
7. Guo, J. et al. Light-driven fine chemical production in yeast biohybrids. *Science* **362**, 813–816 (2018).
8. Wu, C., Li, T., Liao, C., Li, L. & Yang, J. Tea polyphenol-inspired tannic acid-treated polypropylene membrane as a stable separator for lithium-oxygen batteries. *J. Mater. Chem. A* **5**, 12782–12786 (2017).
9. Huang, S., Li, X., Jiao, Y. & Shi, J. Fabrication of a superhydrophobic, fire-resistant, and mechanical robust sponge upon polyphenol chemistry for efficiently absorbing oils/organic solvents. *Ind. Eng. Chem. Res.* **54**, 1842–1848 (2015).
10. You, F., Xu, Y., Yang, X., Zhang, Y. & Shao, L. Bio-inspired Ni^{2+}-polyphenol hydrophilic network to achieve unconventional high-flux nanofiltration membranes for environmental remediation. *Chem. Commun.* **53**, 6128–6131 (2017).

11. Saowalak, K., Titipun, T., Somchai, T. & Chalermchai, P. Iron(III)-tannic molecular nanoparticles enhance autophagy effect and T_1 MRI contrast in liver cell lines. *Sci. Rep.* **8**, 6647 (2018).
12. Shin, M. et al. Targeting protein and peptide therapeutics to the heart via tannic acid modification. *Nat. Biomed. Eng.* **2**, 304–317 (2018).
13. Shin, J. et al. Three-dimensional electroconductive hyaluronic acid hydrogels incorporated with carbon nanotubes and polypyrrole by catechol-mediated dispersion enhance neurogenesis of human neural stem cells. *Biomacromolecules* **18**, 3060–3072 (2017).
14. Wang, Y. et al. Ultralong circulating lollipop-like nanoparticles assembled with gossypol, doxorubicin, and polydopamine via π–π stacking for synergistic tumor therapy. *Adv. Funct. Mater.* **29**, 1805582 (2019).
15. Yang, Z. et al. Metal-phenolic surfaces for generating therapeutic nitric oxide gas. *Chem. Mater.* **30**, 5220–5226 (2018).
16. Yang, C. S., Sang, S., Lambert, J. D. & Lee, M. J. Bioavailability issues in studying the health effects of plant polyphenolic compounds. *Mol. Nutr. Food Res.* **52**, S139–S151 (2008).
17. Shavandi, A. et al. Polyphenol uses in biomaterials engineering. *Biomaterials* **167**, 91–106 (2018).
18. Sadeghi-Ghadi, Z. et al. Potent in vitro activity of curcumin and quercetin co-encapsulated in nanovesicles without hyaluronan against Aspergillus and Candida isolates. *J. Mycol. Med.* **30**, 101014 (2020).
19. Mihoub, A. B. et al. Synthesis of new water soluble β-cyclodextrin@curcumin conjugates and in vitro safety evaluation in primary cultures of rat cortical neurons. *Int. J. Mol. Sci.* **22**, 3255 (2021).
20. Krogsgaard, M., Nue, V. & Birkedal, H. Mussel-inspired materials: Self-healing through coordination chemistry. *Chem. Eur. J.* **22**, 844–857 (2016).
21. Song, J. et al. Mechanically and electronically robust transparent organohydrogel fibers. *Adv. Mater.* **32**, 1906994 (2020).
22. Meredith, H. J. & Wilker, J. J. The interplay of modulus, strength, and ductility in adhesive design using biomimetic polymer chemistry. *Adv. Funct. Mater.* **25**, 5057–5065 (2015).
23. Westwood, G., Horton, T. N. & Wilker, J. J. Simplified polymer mimics of cross-linking adhesive proteins. *Macromolecules* **40**, 3960–3964 (2007).
24. Zhu, H. et al. Facile and green synthesis of well-dispersed Au nanoparticles in PAN nanofibers by tea polyphenols. *J. Mater. Chem.* **22**, 9301–9307 (2012).
25. Fei, J. et al. One-pot ultrafast self-assembly of autofluorescent polyphenol-based core@shell nanostructures and their selective antibacterial applications. *ACS Nano* **8**, 8529–8536 (2014).
26. Wang, J., Wang, Y. & Li, Q. Synthesis of AuNPs using plant polyphenols and their potential treatment for age-related macular degeneration. *J. Drug Deliv. Sci. Tec.* **55**, 101377 (2020).
27. Chavva, S. R. et al. Epigallocatechin gallate-gold nanoparticles exhibit superior antitumor activity compared to conventional gold nanoparticles: Potential synergistic interactions. *Nanomaterials* **9**, 396 (2019).
28. Zhang, X. L. et al. One-pot synthesis of gold nanostars using plant polyphenols for cancer photoacoustic imaging and photothermal therapy. *J. Nanopart. Res.* **18**, 174 (2016).
29. Jin, R., Zeng, C., Zhou, M. & Chen, Y. Atomically precise colloidal metal nanoclusters and nanoparticles: Fundamentals and opportunities. *Chem. Rev.* **116**, 10346–10413 (2016).
30. Chakraborty, I. & Pradeep, T. Atomically precise clusters of noble metals: Emerging link between atoms and nanoparticles. *Chem. Rev.* **117**, 8208–8271 (2017).
31. Wang, Z. et al. The synergy between natural polyphenol-inspired catechol moieties and plant protein-derived bio-adhesive enhances the wet bonding strength. *Sci. Rep.* **7**, 9664 (2017).
32. Wang, F. et al. Solubilization of phloretin via steviol glycoside-based solid dispersion and micelles. *Food Chem.* **308**, 125569 (2020).
33. Prakash, D., Upadhyay, G., Pushpangadan, P. & Gupta, C. Antioxidant and free radical scavenging activities of some fruits. *J. Complement. Integr. Med.* **8**, 1–16 (2011).
34. He, Y., Lin, Y., Li, Q. & Gu, Y. The contribution ratio of various characteristic tea compounds in antioxidant capacity by DPPH assay. *J. Food Biochem.* **44**, e13270 (2020).
35. Kostyuk, V. A., Potapovich, A. I., Suhan, T. O., de Luca, C. & Korkina, L. G. Antioxidant and signal modulation properties of plant polyphenols in controlling vascular inflammation. *Eur. J. Pharmacol.* **658**, 248–256 (2011).
36. Yang, C. Y. et al. Polyphenols isolated from Xanthoceras sorbifolia husks and their anti-tumor and radical-scavenging activities. *Molecules* **21**, 1694 (2016).
37. Zhao, Y. et al. The beneficial effects of quercetin, curcumin, and resveratrol in obesity. *Oxid. Med. Cell Longev.* **2017**, 1459497 (2017).
38. Mandel, S. A., Amit, T., Weinreb, O. & Youdim, M. B. H. Understanding the broad-spectrum neuroprotective action profile of green tea polyphenols in aging and neurodegenerative diseases. *J. Alzheimers Dis.* **25**, 187–208 (2011).
39. Russo, G. L. et al. Mechanisms of aging and potential role of selected polyphenols in extending healthspan. *Biochem. Pharmacol.* **173**, 113719 (2020).